Long-period MT data were collected at 69 stations along the two transects Warumpi and Amadeus (Figure 2). Instrumentation consisted of five-component MT instruments, each measuring three orthogonal magnetic components (B_x, B_y and B_z) and two orthogonal electric components (E_x, and E_y). Magnetic fields were measured using a fluxgate magnetometer and electrodes were porous copper/copper sulphate pots. The survey was carried out under an assumption that the region is electrically 2D, such that resistivity changes with depth and across strike but not along strike. In 2D settings MT data decompose into two independent modes: the transverse electric (TE) mode, where the electric axis is parallel to strike and the transverse magnetic (TM) mode, where the electric axis is perpendicular to strike (Simpson and Bahr, 2005).

The 140-km-long Warumpi transect contains 33 stations and data at most stations were recorded for approximately 2 days. A full description and interpretation of this transect is given in Selway et al. (2006). Data were collected at 36 stations along the 22-km-long Amadeus transect, which links with the Warumpi transect in the north and extends to the northern Musgrave Block in the south. Data at most stations were recorded for approximately 3 days.

MT impedances and jackknife error estimates were determined using the code Robust Remote Reference Magnetotellurics (RRRMT) (Chave et al., 1987). This produced impedance estimates in the period range ~10s to 2000s in the Warumpi transect and ~10s to 4000s in the Amadeus transect.

Station magnetic field data were remote referenced either with magnetic observatory data from Alice Springs or with data from a simultaneously recording station to improve the signal to noise ratio.

Although surface geology in the southern Arunta region supports a 2D assumption with a consistent, approximately E-W strike, the deeper geoelectric structure may be significantly more complex. Any 3D structures that do exist may produce spurious model features if modelled with a 2D code, so dimensionality of the region was tested. Warumpi profile stations were analysed using the phase-sensitive skew (Bahr, 1988). Results of these analyses resulted in 7 sites being identified as either 3D or of poor quality and not included in modelling, as described in Selway et al. (2006). Data from the Amadeus profile were analysed with the phase tensor (Caldwell et al., 2004), which demonstrated that the majority of stations are electrically 2D.

Data from all stations were additionally analysed using the Lilley angle technique (Lilley, 1998) which evaluates dimensionality by comparing the individual strike directions of the real and imaginary parts of both the electric and magnetic fields at each period. The magnetic field strike represents the regional geoelectric strike and should therefore be consistent in a 2D setting. Strike directions obtained from magnetic Lilley angles from all stations are shown on Figure 3. Strike is at approximately N100ºE along most of the profile, which is in very good agreement with strike directions of structures produced in the major intracratonic Palaeozoic Petermann and Alice Springs Orogenies. The strike direction changes at the three southernmost stations on the profile to ~N45ºE, representing electrical 3-dimensionality, so these stations were not included in modelling. Three stations from the Amadeus transect were excluded from modelling since animal interference during data collection resulted in them each having only one electric channel, so a full dimensionality analysis was impossible. All other data points not conforming to 2-dimensional behaviour with a strike approximating N100ºE were also excluded from the inversion.

2D data from the Warumpi and Amadeus transects were modelled together along a single 360 km long profile with bearing of N10ºE using the Non-Linear Conjugate Gradients (NLCG) algorithm (Rodi and Mackie, 2001). TE and TM modes, together with the vertical magnetic field (Hz) were jointly inverted. To account for static shift effects, static shift was included as a parameter to be inverted and the apparent resistivity error floors were set at 30% while phase error floors were 1.45º and Hz error floors were 0.1. A starting half-space of 700 Ωm was determined to be ideal to image distinct model features while minimising artefacts. The inversion code contains a parameter (tau) that acts as a trade-off between model smoothness and data fit (Rodi and Mackie, 2001). Models were run at tau values of 1, 3, 5 and 10 to test which features were sufficiently required by the data that they remained even when model smoothness was emphasised. Three features were required by the data by this measure and are labelled A, B and C on the final model section shown in Figure 4. This model has a tau of 3 and inverted to an rms of 2.4. The rms of the model fit at each of the stations is shown in Figure 4 and the model fit of four stations spaced along the profile is shown in Figure DR1.

The modelled southerly dip between features B and C is particularly important for the geological interpretation of this model and was therefore tested with further model appraisals. Models were produced by individually inverting the TM, TE and Hz subsets of data to determine whether the dip is required by all subsets. Models inverted from TM and TE data each show the same dominant features (A, B and C) as the full-component model, including the southerly dip between regions B and C. Since the TE-mode electric field is measured across strike and is not affected by current gathering, boundaries between the regions were less distinct for the TE only model. The main feature of the model produced by inverting only Hz data is a low-resistivity zone beneath the Amadeus Basin, beginning at a depth of approximately 40km, with no south-dipping boundary evident. Hz data have significantly less resolution of features than MT data and also respond to broader, more distant features. The absence of a south-dipping boundary in this model does not therefore call the existence of the boundary into question. Instead, the features modelled show that the Hz data are less important than the TE and TM data in the full-component model.

Two further model tests were run to assess the robustness of the southerly dip of the boundary between regions B and C. In the first, the final model (Figure 4) was edited such that the boundary had a vertical dip, extending down from the boundary between the Warumpi Province and the NAC at the surface. The forward model produced an rms of 3.4. When allowed to invert, features similar to the original southerly dip resulted. The second test was for a northerly dip and the model was similarly edited such that the boundary between the Warumpi Province and the NAC dipped north at approximately 45˚. The forward model produced an rms of 3.3 and features similar to the original southerly dip were again produced when the model was allowed to invert. The higher rms values of the forward models show that the data are not fit as accurately by northerly or vertical-dipping boundaries. The appearance in the inversions of features similar to those in Figure 4 shows that these features are required to most accurately fit the data. These tests suggest that the southerly dip between regions B and C is a robust feature that is required by the data.

Figure

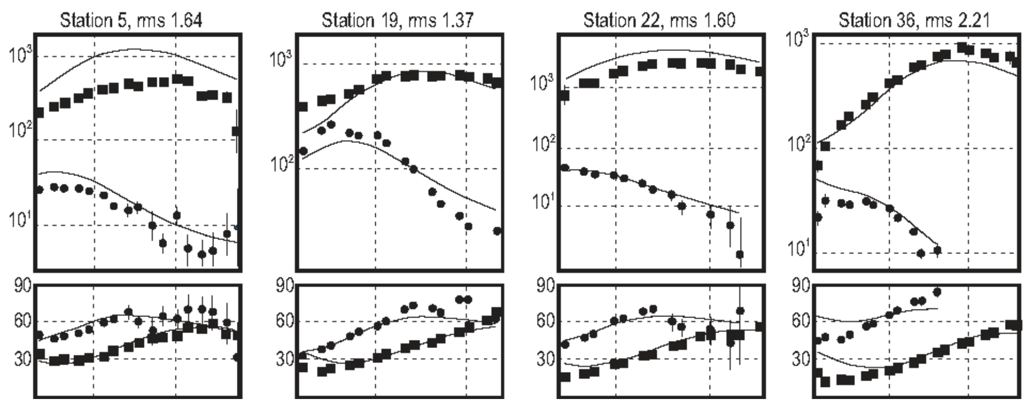

Figure DR1. Station and model data at stations 5, 19, 22 and 36. Rectangles represent the TE mode and circles represent the TM mode. Data points not included in modelling due to three-dimensionality are not shown. Fixed-value offsets between the station and modelled data are due to the static shift correction.

References Cited

Bahr, K., 1988, Interpretation of the magnetotelluric impedance tensor: Regional induction and local telluric distortion: Journal of Geophysics, v. 62, p. 119–127.

Chave, A.D., Thompson, D.J., and Ander, M.E., 1987, On the robust estimation of power spectra, coherences and transfer functions: Journal of Geophysical Research, v. 92, p. 633–648, doi: 10.1029/JB092iB01p00633.